Nanotechnology Perceptions
ISSN 1660-6795
www.nano-ntp.com

Investigation of ITO/MEH-PPV/PEDOT:PSS/Ag heterostructure based Organic Light Emitting Diode: Structure, Numerical analysis and Simulation

Shalini Jharia[1], Pravendra Tyagi[2], Seema Agrawal[2]

[1]Department of Physical Sciences, Banasthali Vidyapith, Rajasthan, India
[2]Electrical Engineering Department, Rajasthan Technical University, Akelgarh, Kota, India

The paper reports electrical and optical characteristics of bilayer organic light emitting diode structure, glass/ITO/MEH-PPV/PEDOT:PSS/Ag. The optoelectronics simulation of the double layer OLED is performed using ATLAS tool. Poly [2-methoxy-5-(2'-ethyl-hexyloxy)- 1,4-phenylene vinylene]) (MEH-PPV) as an EL (emissive layer) and Poly (3,4-ethylene dioxythiophene) -poly (styrene sulfonate)(PEDOT:PSS) as a ETL (electron transport layer) are used in OLED. The behavior of electron transport layer, PEDOT:PSS studied, which allows transfer of electrons from silver cathode(Ag) to the LUMO (lowest occupied molecular orbital) of MEH-PPV. This increase in electrical injection causes the electroluminescence to increase. In addition, the turn-on voltage of proposed structure is reduced to ~3V. The maximum luminance with 1.9×10-18 W/μm was obtained with MEH-PPV is doped with the p-type semiconductor for the ITO/MEH-PPV/PEDOT:PSS/Ag structure at 10V. And also find the recombination rate and how the anode current changes during short periods of time (about μs).
Keywords: OLED, Atlas, TCAD Silvaco, Active layer, Electron transport layer, PEDOT:PSS, Simulation

1. Introduction

OLEDs (Organic light-emitting diodes) are devices that are suitable for future-generation displays like OLED display with an OS/Si construction with two-dimensionally organized drivers fabricated by (Kozuma et al., 2024).Organic light emitting diodes have garnered significant attention from both scientific research and prominent consumer electronics

companies due to their flexibility and high resolution (Lee et al.,2024), eco-friendliness, high efficiency and ease of fabrication in an ambient temperature setting [Kunić & Šego, 2012; Negi & Kumar, 2018]. Recently magnetic field model for OLED screens and a 3D model for analyzing current and magnetic fields developed [Wang et al., 2024]. Various junctions' interfaces that are important in multilayered OLEDs for both electron and hole injection. During the charge transfer process, these junctions act as obstacles. Here, these barriers lead to increased operating voltages, decreased performance, and expedited OLED breakdown (Xing et al., 2024; Lee & H., 2023). A lower interface barrier is desired for better injection of the charge carriers is important for decreasing power consumption, because the currents are regulated by both the charge transport surface and the charge injection. To emit light, OLEDs necessitate the charge carriers injection from touching electrodes. From anode surface Holes are injected, while electrons are injected from the metallic cathode; hole-electron couple are subsequently recombined at the emission layer (Luscombe et al., 2021).

OLED is categorized as mono layer and double layer by layer count, where transportation, recombination, and emission occur. An extended research added hole transport layer (HTL), hole injection layer (HIL), electron transport layer (ETL), and electron injection layer (EIL) for high-efficiency, high-speed devices. Researchers simulate single layer OLED with PVK-PEDOT organic matrix [Mhamedi et al., 2023] and another predicted the electrical and optical characteristics using P3BEdotBT3A, an organic substance, as the emission layer [El Karkri et al., 2022]. An alternative method is provided by numerical modeling, which assesses how an OLED's capacitive behaviour affects its correct operation. The first stage is to analyse the operation of an OLED and an explanation of the capacitive phenomena, then proceed to a present of their LT-Spice electrical model [Slimani et al., 2023].

Continuation of the expanding research that is being done on OLEDs. Researchers investigated Al-NG complex-based OLED with PEDOT:PSS as hole transporting layer (Chouk et al., 2021). The research outlining the background and methodology of the PEDOT: PSS synthesis (Elschner et al., 2010). Because of its durability, exquisite electrical and optical qualities, and importance in optoelectronic device technology. The PEDOT:PSS is conductivity polymer that is the most widely used and successful. PEDOT:PSS is made up of two polymers. One is Poly (3,4-ethylenedioxythiophene), often known as PEDOT, which is a conjugated polymer with a positive charge and the second polymer is sodium polystyrene sulfonate (PSS), which is sulfonated polystyrene (Gueye et al., 2020; Elschner & Lövenich, 2011). PEDOT:PSS placed between the cathode aluminium (Al) and the emissive layer (EML) MEH-PPV, enhances carrier transportation (Hewidy et al., 2017). PEDOT:PSS has exceptional electrical, optical, and mechanical properties, which widely employed in organic electronics research and OLED applications for high efficiency. The two layers into touch and, consequently, improving the device performance as well as managing the energy disparity between silver and polymer MEH-PPV(Scott et al., 1997; Kugler et al.,1999). MEH-PPV have potential a high stability that allowing easy deposition of the top contact, application uses in inexpensive printable electronics, flexible circuits, and large-area fields of electronic devices [Burroughes et al.,1990; Sekitani et al., 2009; Briseno et al., 2006). However, the efficiency and the conductivity of OLEDs is still far behind the real requirement to simulate. Thus, the more efficient materials layers are highly desired.

This paper reports the simulation of OLED structure made of Glass/ITO/MEH-PPV/

PEDOT:PSS/Ag. The TCAD silvaco tool used to simulate optoelectronics characteristics of OLED. Two organic layers (MEH-PPV and PEDOT:PSS) are used between two electrodes (ITO and silver). Taking into consideration the modelling of the suggested OLED structure with MEH-PPV as the emissive layer and PEDOT:PSS as the electron transport layer. The necessary computations have been executed to ascertain the anticipated electrical and optical properties, including I-V and J-V properties, the behavior of the charge density when biased at 10V. MEH-PPV when added above to PEDOT:PSS, improves the performance of OLED devices.

2. OLED structure specifications and operation

Basically, heterostructure based OLED structure is made of a transparent substrate material such as glass, two electrodes (anode and cathode), organic and semiconductor materials such as PEDOT: PSS represents the ETL. In proposed OLED structure as shown in fig.1(a), PEDOT:PSS organic film is sandwiched between an active layer MEH-PPV, and Ag cathode. Fig.1(b) is the energy band diagram of structure ITO/MEH-PPV/PEDOT:PSS/Ag. Where MEH-PPV is used for carrier emission and PEDOT: PSS is used for carrier transportation. In The transparent ITO (Indian tin oxide) anode usually uses for light visibility. This material is also an excellent conductor with a high work function(4.7eV), which promotes hole injection into the HOMO(-4.9eV) level of MEH:PPV.

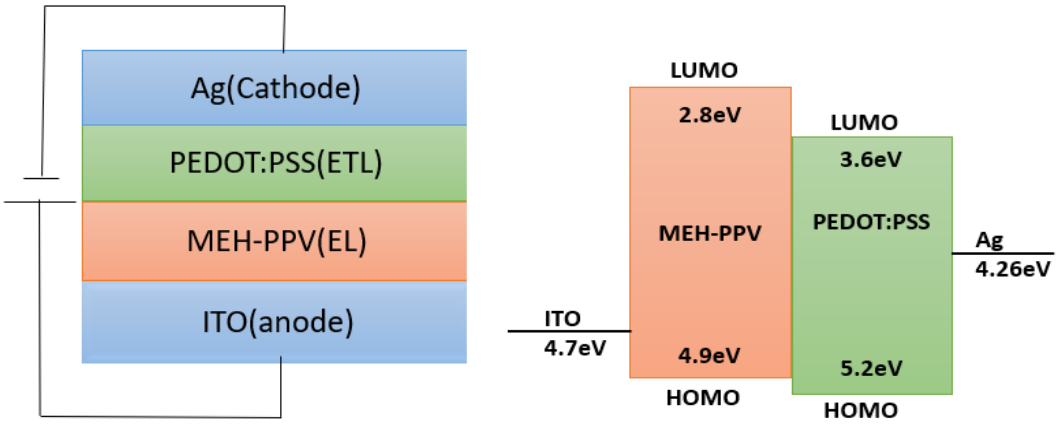

Figure 1(a)ITO/MEH-PPV/PEDOT:PSS/Ag structure of OLEDs (b)Energy band diagram

Similarly Ag can be used to inject electrons into the LUMO (-3.6eV) of PEDOT:PSS. In the application of external potential across OLED, Photons release a specific amount of energy in the form of an exciton when there is a recombination of cathode electrons and anode holes. However, the work function of the electrods (cathode and anode) is really important in operation of OLED. [Udhiarto et al., 2017]. To decrease operating voltage, the cathode work function must be lower than the anode workfunction. The core of the light-producing device, the emissive layer is where the conversion of electrical energy into light occurs.

In the table1. the layers that are utilized to form the OLED structure are illustrated.

Table 1: Material parameters utilized during modeling (Kersenan et al., 2021)

Parameter	MEH-PPV	PEDOT: PSS
Thickness(nm)	50nm	50nm
Affinity, E_a(eV)	2.8	0.673
Hole Mobility,μ_p $(cm^2/V-s)$	$1x10^{-9}$	40
Electron Mobility, $\mu_n(cm^2/V-s)$	$1x10^{-9}$	1
Relative Permittivity, ε_r	3.0	2.2
Density of state for electrons, Nc(cm^{-3})	$2.5x10^{19}$	$2.0x10^{21}$
Density of state for hole, Nv(cm^{-3})	$2.5x10^{19}$	$2.0x10^{21}$
Temperature, T (K)	300	300
Real Index	1.67	-

3. Simulating Method

In this paper 2-Dimensional Atlas simulator TCAD used. It includes a wide range of features for emulating OLEDs. Step-by-step coding can be used for modling and simulation as shown in figure 2. First mashing is done to form OLED structure using the Atlas syntax. The intervals between a sequence of horizontal and vertical lines form a structural mesh. For precise findings and model gain, a good mesh is essential.

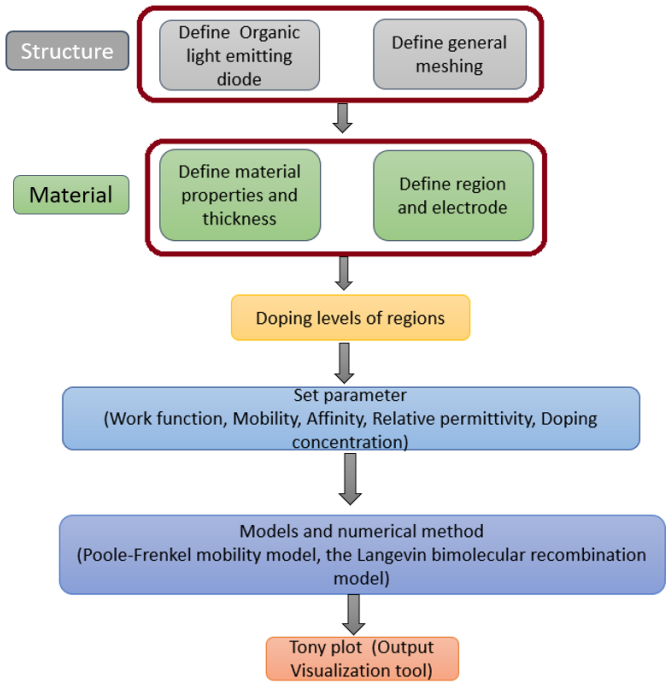

Figure 2: Simulation process of proposed OLED in ATLAS silvaco tool (A.U.S.,&Santa Clara, 2016)

The models Poole-Frenkel and the Recombination Langevin are described below in equations, to fully understand the physical characteristics of organic devices,

$$\mu_n(E) = \mu_{n0} \exp\left(\frac{-DELTAEN.PFMOB}{KTneff} + \left(\frac{BETAN.PFMOB}{KTneff} - GAMMA, PFMOB\right)\sqrt{|E|}\right) \quad \text{-------(1)}$$

$$\mu_p(E) = \mu_{p0} \exp\left(\frac{-DELTAEP.PFMOB}{KTneff} + \left(\frac{BETAP.PFMOB}{KTneff} - GAMMA, PFMOB\right)\sqrt{|E|}\right) \quad \text{--------(2)}$$

Where ΔEN.PFMOB = Energy required for activation in electron, ΔEP.PFMOB= Energy required for activation in holes, μ_{e0}(E)= mobility depend on field, μ_{e0}= Mobility on zero field, βN.PFMOB = Electron Poole-Frenkel factor, βP.PFMOB= Hole Poole-Frenkel factor

The Langevin equation for the recombination rate coefficient is provided below equation:

$$R_L(x,y,t) = ALANGEVIN \frac{q[\mu_n(E) + \mu_p(E)]}{\varepsilon_r \varepsilon_o} \quad \text{---------(3)}$$

$$R_L(x,y,t) = ALANGEVIN \frac{q \min(\mu_p \mu_\rho)]}{\varepsilon_r \varepsilon_o} \quad \text{----------(4)}$$

Where ε_r is relative permittivity of medium, ε_0 is permitivitty of vacuum, A.Langevin is the prefactore for the Langevin bimolecular recombination model. By default, the value of model parameter, A.Langevin is 1.

The Langevin equation of the bimolecular recombination rate are shown in equation:

$$R_L n, p = r_L(x,y,t)(n.p - n_i^2) \quad \text{----------(5)}$$

The mobility model of Poole-Frenkel might lead to convergence issues because of its heavy reliance on the electric field.

To improve the Poole-Frenkel model stability, the expression given below are used.

$$\mu_h(E) = \frac{1}{\frac{1}{\mu_{h_{pf}}(E)} + \frac{1}{\mu_{h_{\lim}}(E)}} \quad \text{----------(6)}$$

$$\mu_e(E) = \frac{1}{\frac{1}{\mu_{e_{pf}}(E)} + \frac{1}{\mu_{e_{\lim}}(E)}} \quad \text{----------(7)}$$

The Drift diffusion current Equation are given below

$$J_e = q_e \mu_e E_e + qD_e \nabla_e \quad \text{----------} \quad (8)$$

$$J_h = q_h \mu_h E_h + qD_h \nabla_h \quad \text{----------} \quad (9)$$

Where J_e and J_h are charge densities, μ_h (E) and μ_e (E) are mobilities for electrons and holes, D_e, D_h the coefficient of diffusion for electrons and holes respectively. The distribution of singlet excitons is utilized to calculate the radiative rates of luminescence in an OLED. The electron and hole drift diffusion equations, as well as the exciton continuity equations, are solved in Atlas.

4. Results and Discussion

To determine the optoelectronics property of the ITO/MEH-PPV/PEDOT:PSS/Ag based OLED structure, initially, the meshing structure is showing in Figure 3, where Ag and ITO added with thickness of 10nm and MEH-PPV and PEDOT:PSS with 50nm thickness. Proper meshing can also lead to electrical results.

The Langevin recombination rate for the OLEDs at 10V is given in figure 4(a),4(b). One of the most fundamental aspects of light emission is the recombination rate of charge carriers.

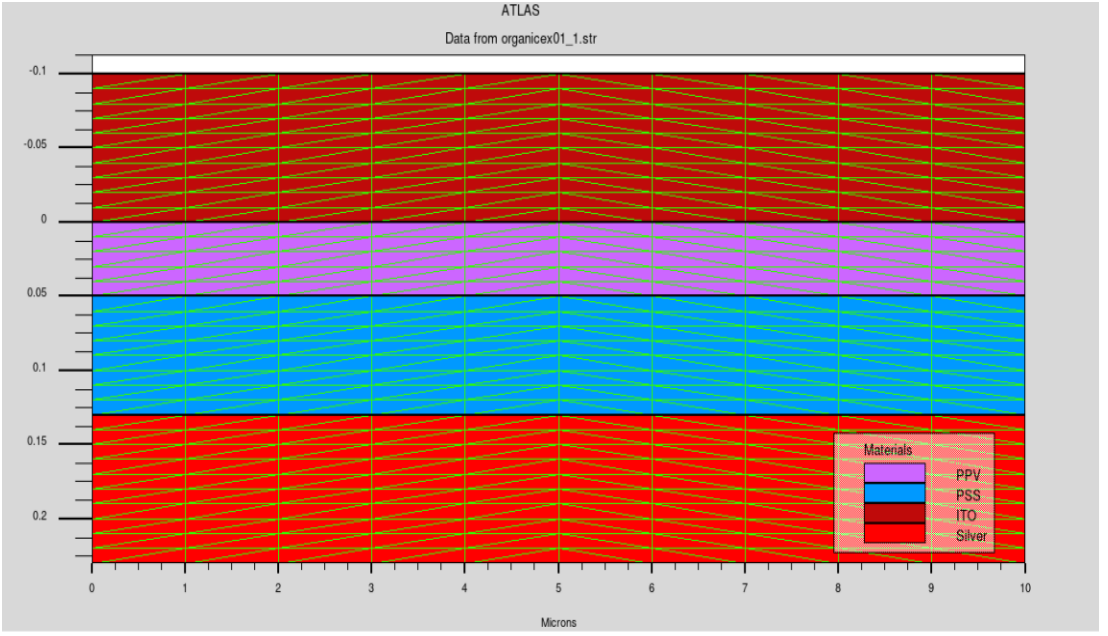

Figure 3 Meshing structure of ITO/MEH-PPV/PEDOT:PSS/Ag

The ability of electrons and holes to move freely and the permittivity of the materials are essential to its operation. The recombination rate increases with the addition of more layers in OLEDs with high permittivity. Increasing the pace at which electrons and holes recombine

results in an increase in the production of excitons. Radiative recombination of injected free carriers occurs in the ETL, from the interface, of the Emissive Layer (EML) (S. Sato et al.,2019). In such a scenario, the electron-transporting layer will be the primary location for electron-hole recombination.

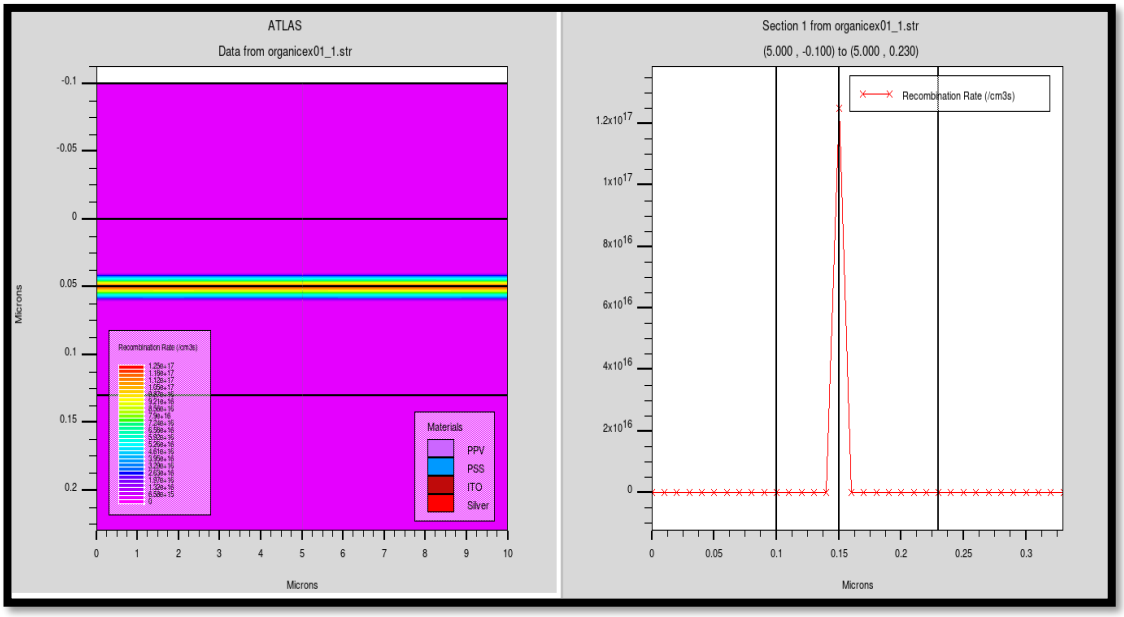

(a) (b)

Figure 4(a) Langevin recombination rate (b) Langevin Recombination rate versus distance along the OLED structure

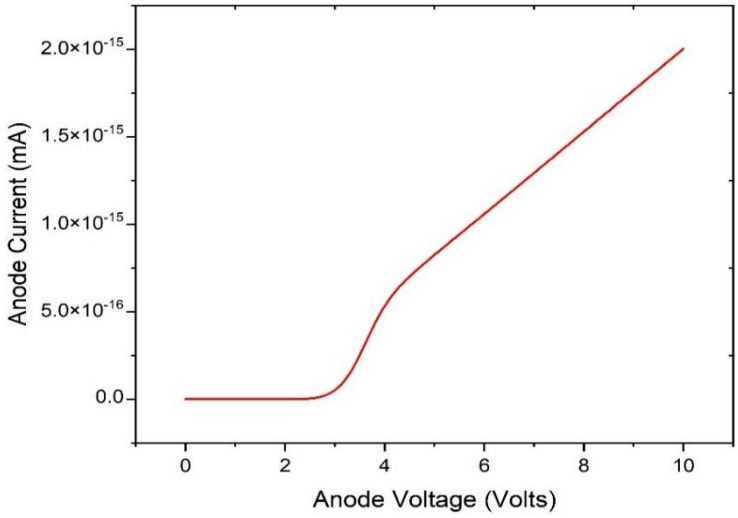

Figure 5. Voltage-current characteristics

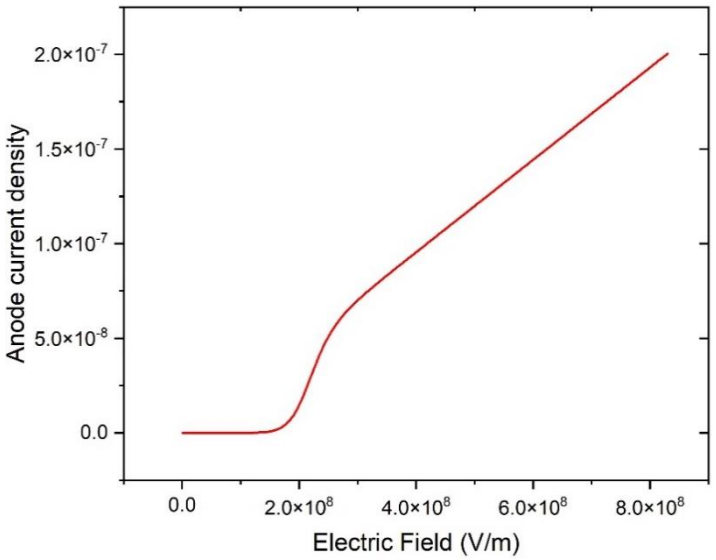

Figure 6. Electrical field versus anode current

The voltage (V)- current (I) characteristic of the OLED, mapped and observed in Figure 5. The turn-on voltage of the OLED obtained approximately ~3.25 V, after this threshold voltage, the electrical current increases rapidly. The energetic interface barriers, which control the release of free holes into the recombination zone and the confinement of electrons in PEDOT:PSS, also have a significant impact on the current. Figure 6. Shows the response of anode current with electrical field. Figure 7 shows luminescent power 2.0x10-^{15}W/um with anode voltage at10volts obtained. The investigation is shows that multilayered structure of OLED is promising technology to improve efficiency of OLED.

Similar, findings for the singlet exciton density shown in Figure 8 It is only possible to anticipate radiative decay from a singlet exciton due to the fact that the Langevin recombination leads to the creation of singlet and triplet excitons through the emission of fluorescent light. The exciton diffuses from the high to low concentration, and will be extended from the interface EL/ETL and forming the emitting zone [Wei, 2010].

The energy expression of exciton which emits a photon, the color of the light emitted may be chosen (Hung & Chen, 2002):

$\Delta E = hc/\lambda$ ----------(10)

where: λ is the emission wavelength. h is the Planck constant (6.626.10^{-34} J.S)

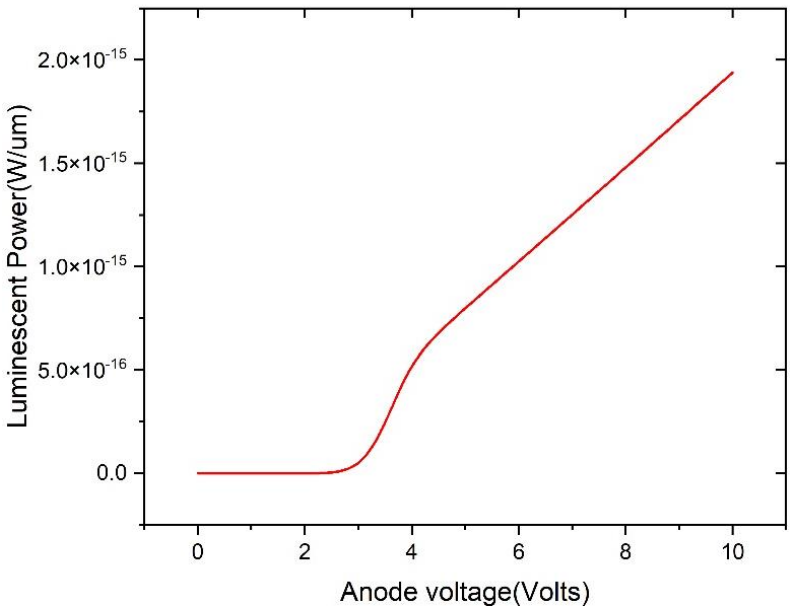

Figure 7. Anode voltage versus luminescent

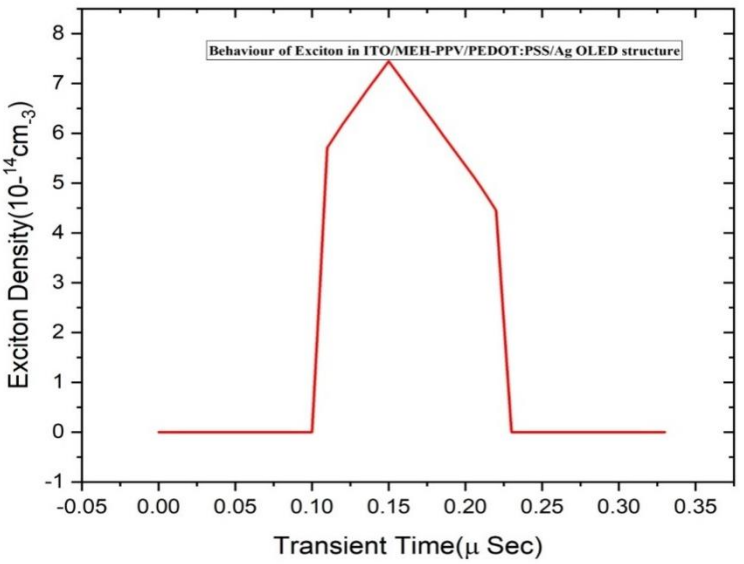

Figure 8. Illustration of exciton density power with transient time.

5. Conclusion

The work study the simulation of OLED ITO/MEH-PPV/PEDOT:PSS/Ag architecture and an approach to numerical simulation of injection-limited OLEDs was proposed. Optoelectronics

characteristics are determined by using OLED simulation with the Silvaco TCAD software. The voltage-current characteristics, recombination rate, transient time relative to anode current curve and the transient time versus exciton density curve are obtained. The model of Langevin recombination consists of solving differential equations and explaining the recombination mechanism, as well as hole and electron mobility. This could be ascribed to PEDOT:PSS serving as ETL that improved the balance of electron and hole current. It resulted in stability and luminescent power of the OLEDs. Additionally, enhance the electrical and electroluminescence capabilities of the device. A significant challenge is the incomplete understanding of the impacts on the electrical properties of organic optoelectronics, equipment, including remove charge carriers after exciton dissociation.

References

1. Kozuma, M., Komura, Y., Miyata, S., Okamoto, Y., Tamatsukuri, Y., Inoue, H., ... & Yamazaki, S. (2024). OLED Microdisplay With Monolithically Integrated CAAC-OS FET and Si CMOS Achieved by Two-Dimensionally Arranged Silicon Display Drivers. IEEE Journal of the Electron Devices Society, 12, 187-194.
2. Lee, D., Kim, S. B., Kim, T., Choi, D., Sim, J. H., Lee, W., ... &Yoo, S. (2024). Stretchable OLEDs based on a hidden active area for high fill factor and resolution compensation. Nature Communications, 15(1), 4349.
3. Kunić, S., &Šego, Z. (2012). OLED technology and displays. In Proceedings ELMAR-2012 (pp. 31-35). IEEE.
4. Negi, S., Mittal, P., & Kumar, B. (2018). Impact of different layers on performance of OLED. Microsystem Technologies, 24, 4981-4989.
5. Wang, H., Feng, X., Yang, A., He, A., Zhang, Z., & Kong, X. (2024). The Simulation of OLED Current Detection Based on Scanning SQUID Microscope. IEEE Transactions on Applied Superconductivity.
6. Xing, X., Wu, Z., Sun, Y., Liu, Y., Dong, X., Li, S., & Wang, W. (2024). The Optimization of Hole Injection Layer in Organic Light-Emitting Diodes. Nanomaterials, 14(2), 161.
7. Lee, H. (2023). Thickness Dependence of MoO3 Hole Injection Layer on Energy-Level Alignment with NPB Hole Transport Layers in OLEDs. Applied Science and Convergence Technology, 32(3), 73-76.
8. Tanghe, G., Thielemans, R., &Dedene, N. (2007). U.S. Patent No. 7,262,753. Washington, DC: U.S. Patent and Trademark Office.
9. Hewidy, D., Gadallah, A. S., & Fattah, G. A. (2017). Electroluminescence enhancement of glass/ITO/PEDOT: PSS/MEH-PPV/PEDOT: PSS/Al OLED by thermal annealing. Journal of Molecular Structure, 1130, 327-332.
10. Luscombe, C. K., Maitra, U., Walter, M., & Wiedmer, S. K. (2021). Theoretical background on semiconducting polymers and their applications to OSCs and OLEDs. Chemistry Teacher International, 3(2), 169-183.
11. Mhamedi, I. E., Karkri, A. E., Malki, Z. E., &Bouachrine, M. (2023). Simulation and analysis of electro-optical characteristics of organic compounds in organic light-emitting diodes(OLEDS). International Journal of Engineering Science Technologies,7(3), 8-22.
12. El karkri, A., El mhamedi, I., & El malki, Z. (2022). Prediction and Simulation of electrical and optical characteristics of an OLED based on P3BEdotBT3A organic material. In E3S Web of Conferences (Vol. 336, p. 00062). EDP Sciences.
13. Slimani, H., Bendaoud, A., Reguig, A., Zeghoudi, A., Tilmatine, A., & Canale, L. (2023, June). Parametric Modeling of the Capacitive Phenomenon in an OLED Excited by Transient Voltage. In 2023 IEEE Sustainable Smart Lighting World Conference & Expo (LS18) (pp. 1-5). IEEE.

14. Chouk, R., Bergaoui, M., Aguir, C., Mhadhbi, M., Bouzidi, C., & Khalfaoui, M. (2021). Numerical Simulation and Performance Enhancement of Organic Light Emitting Diodes Based on Ninhydrin-Glycine Schiff Base Materials. IEEE Electron Device Letters, 43(1), 120-123.
15. Elschner, A., Kirchmeyer, S., Lovenich, W., Merker, U., & Reuter, K. (2010). PEDOT: principles and applications of an intrinsically conductive polymer. CRC press.
16. Gueye, M. N., Carella, A., Faure-Vincent, J., Demadrille, R., & Simonato, J. P. (2020). Progress in understanding structure and transport properties of PEDOT-based materials: A critical review. Progress in Materials Science, 108, 100616.
17. Hewidy, D., Gadallah, A. S., & Fattah, G. A. (2017). Electroluminescence enhancement of glass/ITO/PEDOT: PSS/MEH-PPV/PEDOT: PSS/Al OLED by thermal annealing. Journal of Molecular Structure, 1130, 327-332
18. Elschner, A., &Lövenich, W. (2011). Solution-deposited PEDOT for transparent conductive applications. MRS bulletin, 36(10), 794-798.
19. Scott, J. C., Carter, S. A., Karg, S., & Angelopoulos, M. (1997). Polymeric anodes for organic light-emitting diodes. Synthetic Metals, 85(1-3), 1197-1200.
20. Kugler, T., Salaneck, W. R., Rost, H., & Holmes, A. B. (1999). Polymer band alignment at the interface with indium tin oxide: consequences for light emitting devices. Chemical Physics Letters, 310(5-6), 391-396.
21. Burroughes, J. H., Bradley, D. D., Brown, A. R., Marks, R. N., Mackay, K., Friend, R. H., ... & Holmes, A. B. (1990). Light-emitting diodes based on conjugated polymers. nature, 347(6293), 539-541.
22. Sekitani, T., Yokota, T., Zschieschang, U., Klauk, H., Bauer, S., Takeuchi, K., ... & Someya, T. (2009). Organic nonvolatile memory transistors for flexible sensor arrays. Science, 326(5959), 1516-1519.
23. Briseno, A. L., Mannsfeld, S. C., Ling, M. M., Liu, S., Tseng, R. J., Reese, C., ... & Bao, Z. (2006). Patterning organic single-crystal transistor arrays. Nature, 444(7121), 913-917.
24. Krautz, D., Lunedei, E., Puigdollers, J., Badenes, G., Alcubilla, R., & Cheylan, S. (2010). Interchain and intrachain emission branching in polymer light-emitting diode doped by organic molecules. Applied physics letters, 96(3).
25. Kumar, A., Bhatnagar, P. K., Mathur, P. C., Tada, K., & Onoda, M. (2005). Optical characterization of MEH–PPV/Alq 3 composite films. Journal of materials science, 40(14).
26. Udhiarto, A., Haryanto, L. M., Khoerun, B., & Hartanto, D. (2017, July). Effect of anode and cathode workfunction on the operating voltage and luminance of a single emissive layer organic light emitting diode. In 2017 15th International Conference on Quality in Research (QiR): International Symposium on Electrical and Computer Engineering (pp. 65-68). IEEE.
27. Kersenan, T., Zakaria, N. F., Shaari, S., Sabani, N., Juhari, N., Ahmad, M. F., & Rahim, A. F. A. (2021). Optimization of MEH-PPV Based Single and Double-Layer TOLED Structure by Numerical Simulation. International Journal of Nanoelectronics & Materials, 14.
28. Manual, A. U. S., & Santa Clara, C. A. (2016). ATLAS user's manual. USA: Silvaco International, 1.
29. Sato, S., Takada, M., Kawate, D., Takata, M., Kobayashi, T., & Naito, H. (2019). Interfacial charges and electroluminescence in bilayer organic light-emitting diodes with different hole transport materials. Japanese Journal of Applied Physics, 58(SF), SFFA02.
30. Wei, M. K., Lin, C. W., Yang, C. C., Kiang, Y. W., Lee, J. H., & Lin, H. Y. (2010). Emission characteristics of organic light-emitting diodes and organic thin-films with planar and corrugated structures. International journal of molecular sciences, 11(4), 1527-1545.
31. Hung, L. S., & Chen, C. H. (2002). Recent progress of molecular organic electroluminescent materials and devices. Materials Science and Engineering: R: Reports, 39(5-6), 143-222